On Visualization and Quantification of Lesion Margin in CT Liver Images

Sami Arıca
Department of Electrical and Electronics Engineering
Çukurova University
Adana, Turkey
arica@cu.edu.tr

Tuğçe Sena Altuntaş
Department of Electrical and Energy
İstanbul Gedik University
İstanbul, Turkey
tugcesenaaltuntas@outlook.com

Gürcan Erbay
Department of Radiology
Başkent University
Adana, Turkey
erbayg@gmail.com

***Abstract*—Cancer is the one of the leading causes of death worldwide, and cancer incidence increases every year. The analysis of lesion margin is quite important to diagnose malignant and benign masses and to detect the presence and the stage of tumor invasion in case of cancer. Accordingly, the aim of the study is to visualize and quantify margin of lesions on radiological images by means of a digital computer. In this study, computed tomography (CT) images of liver have been employed for analysis because the liver has crucial tasks in our body and liver cancer-related deaths is ranked as the forth among the cancer-related deaths. The proposed method consisted of four main steps: image cropping and smoothing, specification of target lesion, the boundary detection of target lesion, and visualization and quantification of margin. First, the images were converted to gray scale. The blank regions surrounding the liver in the CT images were removed before specification of target lesion, and further were smoothed with a bilateral filter. Next, the target region was specified roughly by drawing it manually. The boundary of lesion was more precisely determined with the active contour method employing the sketched borderline as the initial curve. Next, the properties of the target region: the centroid, major axis length, and the orientation values were computed. The intensities along a line passing through the center of the tumor were obtained for eighteen different rotation angles. A pulse model was fit to each of the intensity signal corresponding to a rotation. Then, the intensity change, margin sharpness and width were acquired from the pulse approximation associated to each rotation angle. The level difference provided the intensity change, the slope of edges gave the margin sharpness, and distance between the start and end points of the pulse edge represented margin width. Besides, the inner (core) and outer diameter with respect to angle were also displayed.**

***Keywords*—medical image processing, computer-aided diagnosis, computed tomography, liver image, lesion margin.**

I. Introduction

Cancer is among the leading causes of death worldwide. Early diagnosis is critical for a successful treatment and hence the cancer stage is very important for the patients. In general chemotherapy medication is required if a cancer invasion exists otherwise the tumor is removed with surgical treatment and operation, and survivability potential of the patient is increased. Correspondingly, the margin analysis of lesions is extremely important to diagnose malignant or benign tumors and to determine the presence and stage of invasion. However, diagnosis of cancer and detection of tumor invasion with a subjective assessment is a challenging problem, many of the physicians need pathology results, which require an operation. Accordingly, computer-aided diagnosis (CAD) is required to decrease the number of unnecessary surgery for cancer patients.

978-1-7281-8073-1/20/ $31.00 © 2020 IEEE

In recent years, a few studies have been done on computer-aided margin characterization of lesions for different cancer types such as breast, and lung. These have been summarized in the following. In [1], mass features were extracted including degree of spiculation, margin sharpness, lesion density, and lesion texture from the computer-delineated margin data, and the selected features were merged into an estimated likelihood of malignancy using an artificial neural network on multi-modality images of the breast. The authors of [2] proposed a new mathematical method for measuring the margins of a lesion from a breast magnetic resonance image for to discriminate malignant and benign lesions in the context of a computer-aided detection and diagnosis system. The margin sharpness of lesions on radiological images has been quantified for content-based image retrieval by the researches in [3]. By the authors of the reference [4], computer-based margin analysis of breast sonography was archived for differentiating malignant and benign masses. In [5], a characterization of margin sharpness was accomplished to determine benign or malignant masses for breast cancer. 3D margin sharpness analysis was implemented in [6] to characterize pulmonary nodules. Margin sharpness of a pulmonary nodule in lung CT images was evaluated for estimating its malignancy by the authors in [7]. However, the methods diverse and depend on the specific applications and there is not a commonly accepted approach. Therefore, an accurate and automatic detection quantification of lesion margin is still requested to identify malignant or benign tumors and to determine the presence and stage of cancer invasion.

This paper is another attempt for computer–aided description of margin of lesion. The liver is an important part of the body and it has been reported that the liver cancer-related deaths is ranked as the fourth among the cancer related death in accordance to the cancer report [8]. Consequently, the tumors in liver CT images were studied. The intensity variation along a line passing through the centroid of tumor were extracted for different orientations of the line and a pulse model was fit to each intensity change. The core and edge regions were specified from the matched pulses. The proposed methodology differs from the present approaches in terms of the quantification of core and margin of tumor, which were mentioned above.

II. Materials and Method

A. Materials

The proposed algorithm was evaluated on 2-D gray level CT images belonging to patients who have liver cancer or metastases in their livers. The images were obtained from Radiology Department at Başkent University in Adana. The size of the images were 512×512 and resolution has been 1.25 pixel/mm. The images was scaled to $0 - 1$ range (0: black and 1: white). The algorithm was implemented by using Matlab© and its Image Processing Toolbox because of its comprehensive library.

B. Method

The method consists of four main steps: image enhancement, specification of target lesion/region, the boundary detection of target lesion and visualization and quantification of margin. The block diagram of the algorithm is sketched in Figure 1. These steps are summarized in the following.

Radiological Images
↓
Image Enhancement
↓
Specification of Target Lesion
↓
The Boundary Detection of Target Lesion
↓
Visualization and Quantification of Margin

Fig. 1: Block diagram of the study

Initially, the RGB images used in the study were converted to gray image by computing Y channel of YCbCr (or NTSC) color space. Firstly, blank regions surrounding the liver of a CT image was removed before specification of target lesion. A threshold was applied to the image to isolate the liver (threshold level was chosen 0.035). The image opening and then closing operations were applied to remove regions smaller than 5×5 pixels and to tear off regions connected less than 5×5 pixels. The connected component with the biggest area was chosen and its bounding box is computed. The image is cut from this bounding box. Then, edge-preserving smoothing was done to achieve a uniform spatial distribution for cropped image. A Gaussian bilateral filter with mask size 7×7 was employed for smoothing. The standard deviation of spatial-domain and intensity-domain of the filter was fixed as 3 and 0.25 respectively.

Next the region of interest was determined loosely by drawing a curve around the tumor manually. This contour was employed as the initial curve for the active contour algorithm. The final lesion boundary was determined automatically running the edge-based active contour method [9]. The initial contour was evolved and located the perimeter of the tumor. And therefore the region of interest was decided.

Following, the centroid, major axis length and the orientation of the region of interest were calculated. Along the major axis, from L pixels left to L pixels right of the centroid, the intensities were picked up. Considering the centroid as the origin, intensity change along line, from -L pixels to L pixels, passing through the origin in the direction of the major axis was achieved. The line was rotated for θ degree and the intensity signal was recorded. This process was repeated until 180 degree rotation was covered in total. The variable L was chosen *75%* of the major axis length and the rotation angle θ was 10 degree which provided 18 one dimensional intensity distributions.

As a next step a pulse was fit to each intensity distribution corresponding to a certain direction. The pulse model consisted of three levels, linearly falling and rising edges (equation 1). The model was matched by considering the levels and the position of the corners as variables and minimizing the square error between the model, $p(t)$ and original intensity signal, $s(t)$ (equation 2).

$$p(t) = \begin{cases} A & -L < t < D \\ \dfrac{B-A}{D-E}(t-D)+A & D < t < E \\ B & E < t < F \\ \dfrac{C-B}{G-F}(t-E)+B & F < t < G \\ C & G < t < L \end{cases} \tag{1}$$

$$\min_{A,B,C,D,E,F,G} \sum_t (s(t) - p(t))^2 \tag{2}$$

The level differences; $|B - A|$ and $|C - B|$ represent the intensity change of the tumor and the differences $D - E$ and $G - F$ show margin width at an orientation angle α and at the opposite orientation angle $\pi + \alpha$. Correspondingly, the margin sharpness for the orientations α and $\pi + \alpha$ is quantified as $\dfrac{B-A}{D-E}$ and $\dfrac{C-B}{G-F}$ respectively. Additionally, the variables D and G are elements of outer boundary and E and F are members of borderline of the core and therefore the outer diameter is $G - D$ and the inner diameter $F - E$ at the orientation angle α. Mean and standard deviation of intensity change, margin sharpness and width, core and outer diameter were also computed. The plot of the intensity change, margin width and sharpness was obtained with respect to orientation angle and the core and outer boundary were sketched on the image to visually investigate the characteristics of the tumor.

Beside inner and outer diameter with regards to angle was also displayed.

III. Results and Discussion

The approach was demonstrated using a sample image in this section. The liver CT image was first converted to gray scale. In the following, each step of the method has been reported. Figure 2a shows a sample liver image. Figure 2b displays the image after removal of blank area surrounding the liver, and Figure 2c is the smoothed image obtained by applying the bilateral filter.

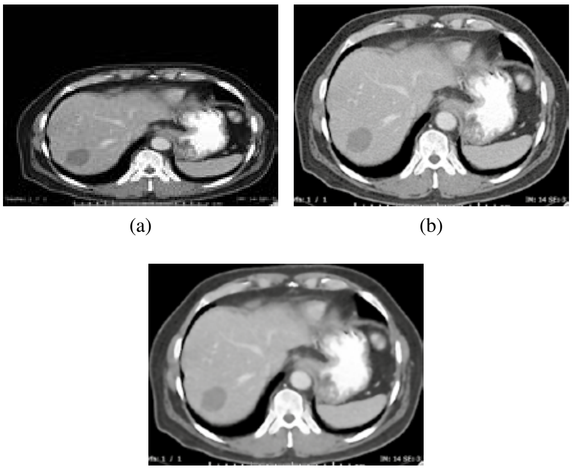

(a) (b) (c)

Fig. 2: (a) Original CT image (b) The cropped image (c) The cropped and smoothed image

The liver image contains a visible lesion (a dark blot on the left). This is a possible tumor and was marked by drawing a contour around it manually as illustrated in Figure 3a.

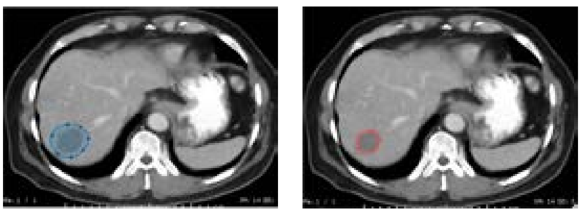

(a) (b)

Fig. 3: (a) Manually specified contour (b) Perimeter of the lesion obtained with active contour method

The contour evolved and moved to the boundary of the lesion by applying the edge-based active contour algorithm. The final loop was excepted as the boundary of the tumor and is indicated in Figure 3b.

From the interior domain of this loop, centroid, major axis length, orientation values were measured. Starting from the direction of the major axis, intensities along lines passing through the centroid were obtained. And for each intensity signal a pulse was fit. The graph of variation for the direction of the major axis is given in Figure 4b. Figure 4c shows the matched pulse. In Figure 4a, the line where intensities of the lesion were read is sketched on the liver image.

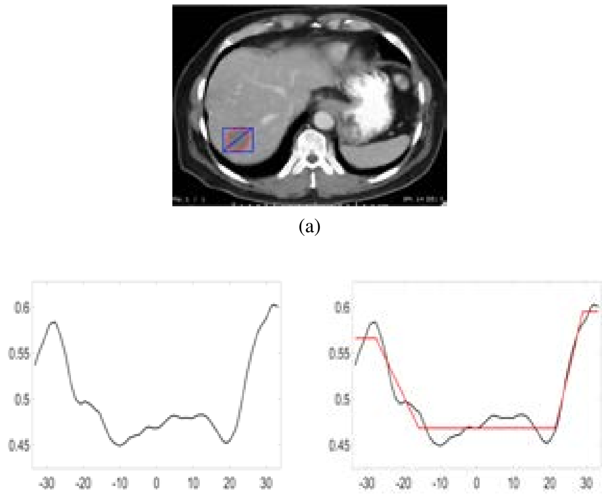

(a) (b) (c)

Fig. 4: a) The line along the major axis direction passing through the centroid b) Pixel values along the line c) The matched pulse to this intensity variation

The intensity change, margin width and sharpness were visualized in one dimension by plotting their graph with respect to directions in Figure 5. The inner and outer diameters were sketched in Figure 6.

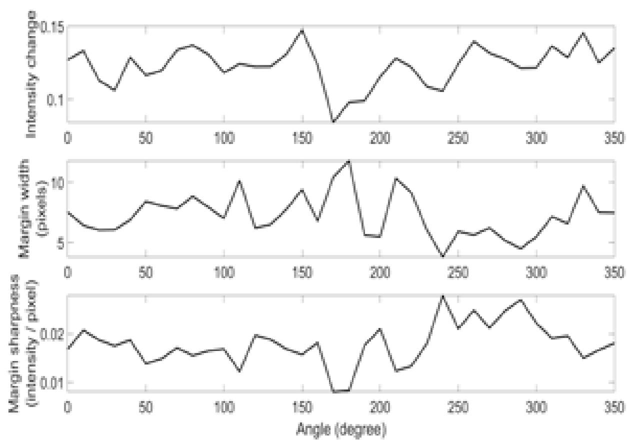

Fig. 5: The plot of intensity change, margin width, and the margin sharpness with respect to angle

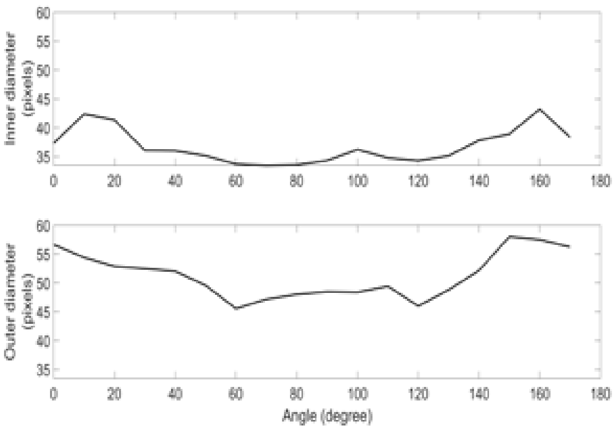

Fig. 6: The plot of inner and the outer diameter with respect to angle

From these graphs given for sample lesion in one CT image in Figure 5 and 6, mean and standard deviations were also were obtained to abstract the characteristics of the tumor. For the sample image, these statistical values are reported in Table I.

TABLE I: The mean and standard deviation values of lesion properties

Lesion Properties	Mean ± Standard Deviation
Intensity difference	0.1231 ± 0.0133
Margin width	7.2741 ± 1.8077
Margin sharpness	0.0179 ± 0.0044
Inner diameter	36.7613 ± 3.0217
Outer diameter	51.3095 ± 3.9791

The limits of core and outer domains were also obtained from the adapted pulse model of each intensity signal. The corner of the falling and rising edges of the adapted pulses provided the inner and outer contour. These loops are given in Figure 7.

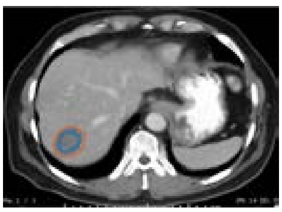

Fig. 7: The boundary of core (inner) and outer region of the lesion

IV. Conclusion

A method for quantification and visualization of tumor margin was proposed to assist a radiologist for diagnosis of malignant and benign masses and detection of the presence and stage of lesion invasion in case of cancer. The surface of the lesion was scanned by rotating a straight line passing through the centroid and reading intensities along the line. The fitted pulse model to the intensity variation of each rotation angle determined the inner and outer domains of the lesion and margin.

This study is a preliminarily study of the semi-automatic or automatic detection and assessment of tumor type (malignant or benign), lesion invasion and their correlation with the specialists' evaluation. As a continuation of this study the approach will be adopted to radiological images other than CT and interpretation of specialists will be picked up and used as a ground truth for estimating tumor characteristics and invasion stage using by the statistical values of lesion. Therefore, comparison with the results of similar studies in the literature has not yet been provided, and also quantitive metrics for evaluating the success of the proposed method have not been defined. The success of the approach will be evaluated after the study is completed.

Acknowledgment

This study was supported by the Scientific Research Project Unit of Çukurova University (Project Number: FDK-2019-11505).

References

[1] N. Bhooshan, M. Giger et al., "Combined Use of T2-Weighted MRI and T1-Weighted Dynamic Contrast–Enhanced MRI in the Automated Analysis of Breast Lesions," Magnetic Resonance in Medicine, 66: 555–563 (2011). 10.1002/mrm.22800

[2] J. E. D. Levman and A. L. Martel, "A Margin Sharpness Measurement for the Diagnosis of Breast Cancer from Magnetic Resonance Imaging Examinations," Acad Radiol, 18: 1577–1581 (2011). 10.1016/j.acra.2011.08.004

[3] J. Xu, S. Napel et al., "Quantifying the margin sharpness of lesions on radiological images for content-based image retrieval," Med. Phys, 39(9): 5405-5418 (2012). 10.1118/1.4739507

[4] C. M. Sehgal, T. W. Cary et al., "Computer-Based Margin Analysis of Breast Sonography for Differentiating Malignant and Benign Masses," J Ultrasound Med, 23(9): 1201–1209 (2004). 10.7863/jum.2004.23.9.1201

[5] C-H. Wei, S. Y. Chen et al., "Mammogram retrieval on similar mass lesions," Computer Methods and Programs in Biomedicine, 106(3): 234-248 (2012). 10.1016/j.cmpb.2010.09.002

[6] A. Felix, M. Oliveira et al., "Using 3D Texture and Margin Sharpness Features on Classification of Small Pulmonary Nodules," In: 29th SIBGRAPI Conference on Graphics, Patterns and Images, pp. 394-400 (2016). 10.1109/SIBGRAPI.2016.58

[7] A. K. Dhara, S. Mukhopadhyay et al., "Quantitative evaluation of margin sharpness of pulmonary nodules in lung CT imagess," IET Image Process., Vol. 10, Iss. 9, pp. 631–637 (2016). 10.1049/iet-ipr.2015.0784

[8] The Global Cancer Observatory (GCO). Cancer Today, Cancer Fact Sheets. http://gco.iarc.fr/today/fact-sheets-cancers [Accessed: 30 Jan. 2020].

[9] V. Caselles, R. Kimmel and G. Sapiro, International Journal of Computer Vision (1997) 22: 61-79. https://doi.org/10.1023/A:1007979827043